Hindawi
Advances in Civil Engineering
Volume 2018, Article ID 7840125, 9 pages
https://doi.org/10.1155/2018/7840125

Research Article

Experimental Study on Explosion Pressure and Rock Breaking Characteristics under Liquid Carbon Dioxide Blasting

Yanan Zhang,[1] **Junren Deng**,[1] **Bo Ke**,[2] **Hongwei Deng**,[1] **and Jielin Li**[1]

[1]*School of Resources and Safety Engineering, Central South University, Changsha 410083, China*
[2]*College of Resources and Environmental Engineering, Wuhan University of Technology, Wuhan 430070, China*

Correspondence should be addressed to Bo Ke; kebo53@163.com and Hongwei Deng; denghw208@126.com

Received 19 April 2018; Revised 17 July 2018; Accepted 26 July 2018; Published 27 August 2018

Academic Editor: Flavio Stochino

A liquid carbon dioxide blasting experiment was carried out under free field conditions, alongside a liquid carbon dioxide rock breaking experiment, to investigate explosion pressure variation and rock breaking characteristics under liquid carbon dioxide blasting. The experimental results show that the internal and external explosion pressures of the liquid carbon dioxide fracturing devices all rapidly increased at first, before attenuating vibrantly after blasting. When the explosion pressure was raised, the internal explosion pressure increased first exponentially and then linearly, while the external explosion pressure increased exponentially throughout. The duration time of the blasting effect stage was about 45 ms. Under the combined effect of jet impingement and a gas wedge of high-pressure carbon dioxide, the rock is subjected to tensile failure. The impact failure and the "gas wedge effect" of high-pressure carbon dioxide play a key role in the rock breaking of liquid carbon dioxide blasting technology.

1. Introduction

In recent years, liquid carbon dioxide blasting technology has attracted significant interest and is now widely used for applications such as increasing the penetration of coal seams [1], gas extraction, urban demolition blasting, and mining [2, 3] as a safe and environmentally friendly blasting technique, but research into the basic theory of liquid carbon dioxide blasting technology currently lags far behind its applications. Operating personnel mainly depend on their prior site experience when using this technology to break rock, rather than using empirically derived concepts, and so it is very difficult to achieve the ideal blasting effect. Furthermore, this approach can cause blasting failure or serious blasting accidents. Therefore, it is particularly important to research the basic theory of liquid carbon dioxide blasting technology.

Research into liquid carbon dioxide blasting technology is currently mainly concentrated in the blasting equipment and its applications. Fong et al. [4] and Elbing et al. [5] designed liquid carbon dioxide blasting equipment, and Pickering [6] introduced the usage of carbon dioxide blasting technology. Guo [7] invented a perfusion machine for filling liquid carbon dioxide fracturing devices. In order to solve a problem whereby existing liquid carbon dioxide fracturing devices can easily fly back when blasting, Yin et al. [8] designed a new carbon dioxide extractor with the function of stopping this fault.

Liquid carbon dioxide blasting technology mainly uses the phase energy of carbon dioxide to achieve its aims [1]. Miller [9] used liquid carbon dioxide blasting technology for cleaning pipelines. Some countries such as Turkey, Russia, and Poland also applied this technology to soften hard coal and control gas [10, 11]. In scenarios where the target rock mass is too fractured to mine, Zhou et al. [12] proposed a mining method that adopted liquid carbon dioxide blasting technology to induce caving. Guo [13] carried out a field test of liquid carbon dioxide blasting the simulated coal. Wang [14] introduced liquid carbon dioxide fracturing technology into the Jiang Zhuang coal mine and greatly improved the efficiency of injecting water in coal seams. Chen et al. [15] found that the radius of the damaged area in a coal body

caused by liquid carbon dioxide blasting technology can reach 5 m and that the permeability of the damaged area increased six-fold after blasting. Lu et al. [16] and Zhou et al. [17] used liquid carbon dioxide blasting technology to increase the permeability of a high gas coal seam and improved the effect of gas extraction significantly; Wang and Xiao [18] used liquid carbon dioxide blasting technology to exploit the marble in a limestone mine and the utilization ratio of the rock was increased significantly. Wang et al. [19] analyzed the hole distribution of liquid carbon dioxide blasting in a coal mine. In addition to these application studies, some experts have also carried out theoretical studies. Dong et al. [20] calculated the TNT equivalence and fractal dimension of liquid carbon dioxide blasting. Kang et al. [21] analyzed the phase transition process of liquid carbon dioxide and calculated the total energy released in this process. Ma et al. [22] analyzed the fractal characteristics and damage effects of the pore structure of specimens frozen by liquid carbon dioxide.

There are few studies on the mechanism of using liquid carbon dioxide for breaking rock. Nilson et al. [23] and Goodarzi [24] used the extended finite element method to simulate the evolution process of cracks in high energy gas fracturing, and proposed a model for predicting crack length. Zhu et al. [25] established the damage mechanics model of high-pressure gas breaking rock and studied the mechanics of crack initiation and propagation at two stages of stress wave and quasistatic. However, these studies are based on the theory of explosive blasting [26, 27], but the variation law of explosion pressure and the rock breaking characteristics of liquid carbon dioxide are not clear.

Here, tests of liquid carbon dioxide blasting under free field conditions, and of rock breaking, are carried out to reveal the variation rule of explosion pressure and the rock breaking characteristics under liquid carbon dioxide blasting and provide the theoretical basis for improving the blasting effect of liquid carbon dioxide blasting technology.

2. Brief Introduction of Liquid Carbon Dioxide Blasting Technology

2.1. Working Principle of Liquid Carbon Dioxide Fracturing Device. The liquid carbon dioxide fracturing device used in this experiment consists of a pneumatic valve, heating device, liquid storage pipe, energy-releasing sheet, sealing gaskets, and a releasing pipe; its structure is shown in Figure 1. The pneumatic valve is used to fill the liquid storage pipe with liquid carbon dioxide. The heating device provides the energy required to transform the liquid carbon dioxide. The liquid storage pipe is used to store liquid carbon dioxide. The energy-releasing sheet controls the maximum explosion pressure of the device. The sealing gasket prevents the leakage of carbon dioxide in the liquid storage pipe, and the releasing pipe controls the release direction of carbon dioxide. When blasting, the heating device is detonated, heating the liquid carbon dioxide; the liquid carbon dioxide then becomes gasified, which increases the pressure in the liquid storage pipe. When the pressure exceeds its maximum shear strength, the energy-releasing sheet is destroyed, quickly releasing the gasified carbon dioxide from the releasing pipe towards the target rock.

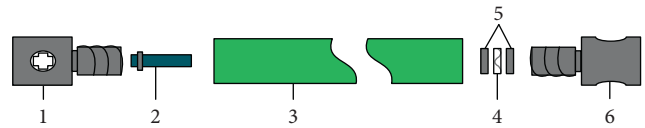

Figure 1: Structural diagram of a liquid carbon dioxide fracturing device. 1: pneumatic valve; 2: heating device; 3: liquid storage pipe; 4: energy-releasing sheet; 5: sealing gaskets; 6: releasing pipe.

2.2. Liquid Carbon Dioxide Filling System. The liquid carbon dioxide filling system consists of a liquid carbon dioxide storage tank, a filling control system, a filling bracket, and a number of connecting pipes; its structure is shown in Figure 2. The liquid carbon dioxide storage tank is used to store liquid carbon dioxide. The filling control system consists of a main switch, a console, a functional area, an operating platform, and other components. The main switch controls the opening and closing of the entire liquid carbon dioxide filling system. The console can also be used to adjust the filling pressure of the liquid carbon. The functional area can be used to manipulate variables such as the filling speed and the weighing filling quality. The operating platform mainly controls the carbon dioxide filling operation. The filling bracket is used to fix the liquid carbon dioxide fracturing device and control its switch.

When filling, the first step is to open valve of the liquid carbon dioxide storage tank ① and the valve of the filling control system ②; this drains the gasified carbon dioxide from the storage tank and the filling system. The next step is to open the valve of the filling bracket ③ and the switch of the fracturing device successively, naturally filling the device with carbon dioxide. Valve ③ is then closed and valve ④ is opened to clean the fracturing device. The filling process is then initiated by closing valve ④, opening valve ③, and pressing the start button. When the set pressure is reached, the filling system is automatically turned off. The valves and main switch of the liquid carbon dioxide filling system are then closed to complete the process.

3. Liquid Carbon Dioxide Blasting Experiment under Free Field Conditions

3.1. Experiment Equipment and Experiment Scheme

3.1.1. The Main Experiment Equipment. Two pieces of experiment were used during the experiment, a liquid carbon dioxide filling system and a dynamic data acquisition system; these are shown in Figures 3 and 4, respectively. The dynamic data acquisition system consisted of a TST6200 transient signal tester manufactured by Chengdu Test Electronic Information Co., Ltd., and piezoelectric pressure sensors with different measuring ranges. The system can collect the internal and external pressure signals of the liquid carbon dioxide fracturing device throughout the process of carbon dioxide blasting.

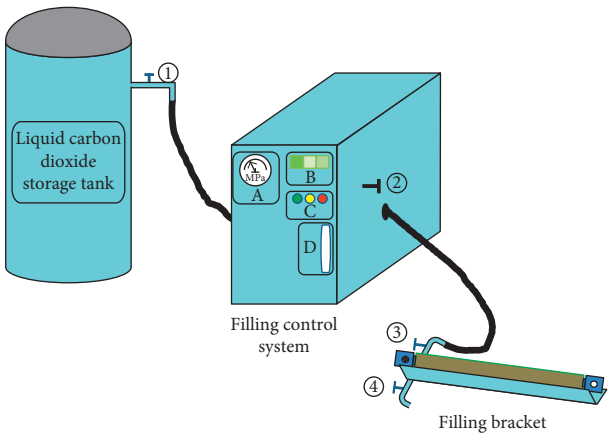

Figure 2: The liquid carbon dioxide filling system. A: console; B: functional area; C: operating platform; D: main switch.

3.1.2. Experiment Scheme. In order to gather the internal and external pressure signals accurately throughout the entire process of liquid carbon dioxide blasting, three pressure sensors with different measuring ranges were placed inside and outside the blasting pipe for the duration of the experiment. The trigger surface of pressure sensor A was inserted into the fracturing device to measure the internal explosion pressure. Pressure sensors B and C were placed outside the fracturing device to measure the external explosion pressure; each pressure sensor was placed the same distance from the air outlet. The arrangement of the pressure sensors and their parameters is shown in Figure 5 and Table 1, respectively. In this experiment, the rated explosion pressure of the energy-releasing sheet was 150 MPa, and the volume of the fracturing device was 48 L.

3.1.3. Equipment Modification. Conventional liquid carbon dioxide fracturing devices are sealed and self-contained, making it impossible to put pressure sensor A in its desired location. In order to measure the internal explosion pressure, the authors redesigned the liquid carbon fracturing device so that the trigger of the sensor could be placed into the interior of the fracturing device. A comparative diagram between the conventional fracturing device and the restructured fracturing device is shown in Figure 6.

In order to protect the fracturing devices, the pressure sensors, and to prevent the fracturing device from throwing during blasting, the authors specially designed experimental equipment suitable for liquid carbon dioxide blasting at free field conditions; its structure is shown in Figure 7 [28]. When blasting, the filled fracturing device is placed in the experimental equipment and fixed by fastening screws, and the pressure sensors that are used to collect the external explosion pressure of fracturing device are attached onto the fixed base and its direction is oriented in a way that is consistent with the outlet direction. The fixed experimental equipment is shown in Figure 8.

3.2. Analysis of the Experiment Results

3.2.1. Analysis of the Explosion Pressure Variation in Fracturing Device. The explosion pressure signals were obtained by the TST6200 transient signal tester and pressure sensor A. These signals need to be filtered to take into account the interference of the stray current, wire arrangement, and other surrounding environmental influences. In this study, a smoothing filter with 16 smooth points was used. After being filtered, the explosion pressure variation of the fracturing device during the entire process of blasting was obtained; it is shown in Figure 9.

Figure 9 shows that the explosion pressure in the fracturing device increased rapidly after the liquid carbon dioxide fracturing device detonated. When the explosion pressure reached the maximum shear strength of the energy-releasing sheet, the energy-releasing sheet was destroyed, and the explosion pressure reached its peak at this point. The explosion pressure then decreased rapidly, and the rate at which the explosion pressure decreased is higher than the rate at which it increased. The explosion pressure in the fracturing device then started to gradually return to atmospheric pressure after the pressure had decreased to its minimum value. In the entire process of liquid carbon dioxide blasting, the duration time from the start of gasifying to full release was 116 ms, and the maximum explosion pressure in fracturing device during this time was 104.62 MPa. The negative pressure zone formed in the later stage of blasting, and the minimum negative pressure was −12.33 MPa. The entire process of liquid carbon dioxide blasting can be divided into three stages: gasification of liquid carbon dioxide, carbon dioxide release, and the recovery of the negative pressure zone.

In order to better analyze the change law of explosion pressure in fracturing device, curves were obtained showing the change in explosion pressure during each of the three stages. The duration time of the first stage, the gasification of liquid carbon dioxide, was 70.04 ms. During this time, the explosion pressure in the fracturing device varied with the rule of "exponential increase followed by linear increase," the early growth rate in the former was much higher than that of the latter. The explosion pressure reached half of its maximum value in 20.3 ms, which is only two sevenths of the liquid carbon dioxide phase transition time. The explosion pressure in the fracturing device followed this rule because the carbon dioxide is liquid, and the explosion pressure in fracturing device is relatively small at the beginning of the blasting process. After energizing the heating device, the heating device generated heat and the liquid carbon dioxide absorbed heat, the carbon dioxide molecule motion then intensified, and the intermolecular spacing increased. Therefore, the liquid carbon dioxide gasified rapidly, and the explosion pressure in the fracturing device increased exponentially. When the explosion pressure in fracturing device increased to a certain point, the heat provided by the heating device had decreased, and the increase in the rate of carbon dioxide molecular motion became relatively stable under the high-pressure action, thus the explosion pressure in the fracturing device increased steadily. When the

(a) (b)

Figure 3: Liquid carbon dioxide filling system.

Figure 4: TST6200 transient signal tester.

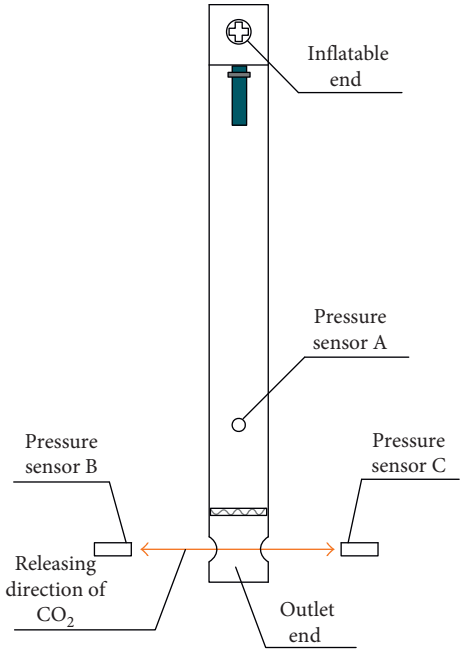

Figure 5: Diagram showing the placement of pressure sensors.

explosion pressure in fracturing device exceeded the shear strength of the energy-releasing sheet, the energy-releasing sheet was destroyed and the gasified carbon dioxide was released at high speed.

The explosion pressure in the fracturing device decreased following the law of oscillatory decay during the second stage, the stage of carbon dioxide release. This means that the explosion pressure decreased rapidly first, then rose again, and repeated several times like this after the energy-releasing sheet was destroyed. There are five peak points in the process of oscillatory decay, and the value of the peak points decreased gradually. The carbon dioxide began to be released at 70.04 ms and continued until 116.44 ms, therefore the entire release time was 46.4 ms. After 9 ms of carbon dioxide release, the explosion pressure in the fracturing device began to fall below 0 MPa. When the pressure in the fracturing device reached its minimum, the explosion pressure in the fracturing device began to parabolically grow and gradually return to the level of atmospheric pressure. The test results also show that the tested maximum explosion pressure in the fracturing device was less than the rated explosion pressure of the energy-releasing sheet.

Table 1: The parameters of the three pressure sensors.

Serial number	Type	Range (MPa)	Sensitivity (Pc/MPa)	Intercept (pC)	Nonlinear (%)
A	MYD-8432C	250	49.077	−105.6	0.20
B(C)	MYD-8432E	40	50.269	−75.3	0.11

(a) (b)

Figure 6: Comparative diagram between the conventional fracturing device and the restructured fracturing device. (a) Conventional liquid carbon dioxide fracturing device. (b) Restructured liquid carbon dioxide fracturing device.

3.2.2. Analysis of the Explosion Pressure Outside of the Fracturing Device. The test results of pressure sensor C were chosen to analyze the variation of explosion pressure outside the fracturing device. Prior to analysis, the test results of the pressure sensor C needed to be filtered. The smoothing filter model with 32 filter points was chosen. Considering that liquid carbon dioxide blasting technology mainly uses high-pressure carbon dioxide, the stage during which the explosion pressure outside the fracturing device is greater than 0 MPa is defined as the liquid carbon dioxide blasting effect stage. In order to better analyze this variation, the change curve of explosion pressure for this stage was amplified; it is shown in Figure 10.

The maximum explosion pressure outside the fracturing device is 5.847 MPa, and the minimum explosion pressure is −0.921 MPa (Figure 10). The liquid carbon dioxide blasting effect stage lasted 45 ms. Overall, the explosion pressure outside the fracturing device increased first and then declined, and the rate at which it increased was higher than that at which it decreased. In the rising stage, the explosion pressure increased exponentially until it reached its maximum. In the falling stage, the explosion pressure did not decrease consistently; it rose again after falling to a certain extent, before declining again. After repeating this pattern several times, the explosion pressure continued to decrease slowly. During the later period of the blasting, the negative pressure zone would have formed in a certain area outside of the fracturing device. After a period of time, this negative pressure zone will disappear. This change law of the explosion pressure outside the fracturing device showed that liquid carbon dioxide blasting technology mainly uses cyclic impacts to work outside at the initial stage of the blasting effect.

The results presented in this paper show that the explosion pressure inside and outside the blasting pipe decreased in an oscillatory fashion. This phenomenon is caused by the outlet structure of the liquid carbon dioxide fracturing device. After the energy-releasing sheet is destroyed, the gasified carbon dioxide will move down at a certain velocity. When the gasified carbon dioxide arrives at the outlet, some of the carbon dioxide will exit the device, whereas some will continue to move down into the lowest level of the device. The explosion pressure in the blasting pipe is always decreasing during this process. When a fraction of the carbon dioxide arrives at the lowest level of the device, the gasified carbon dioxide will be subjected to a reaction from the device. The motion of the gasified carbon dioxide will be hindered, so the explosion pressure in the blasting pipe will increase. After a time, this reaction weakens, and the velocity of the gasified carbon dioxide increases again. Therefore, the explosion pressure in the blasting pipe decreases again. This process repeats several times, leading to the observed

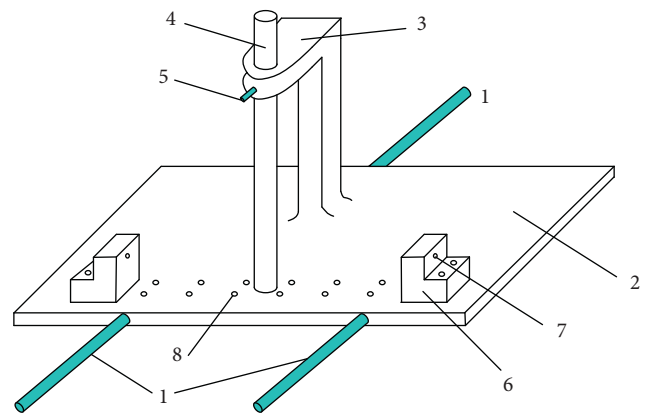

Figure 7: Structural diagram of experiment equipment. 1: support bar; 2: pedestal; 3: backbone; 4: liquid carbon dioxide fracturing device; 5: fastening screw; 6: fixed base; 7: pressure sensor; 8: regulation orifice.

Figure 8: The fixed experimental equipment.

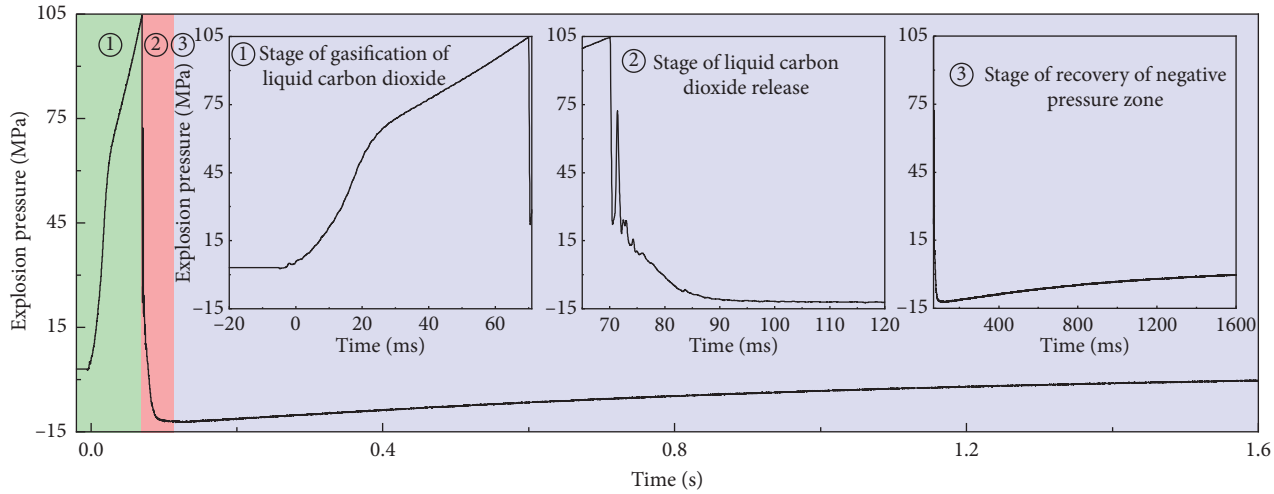

Figure 9: The change line of explosion pressure in fracturing device during entire blasting process.

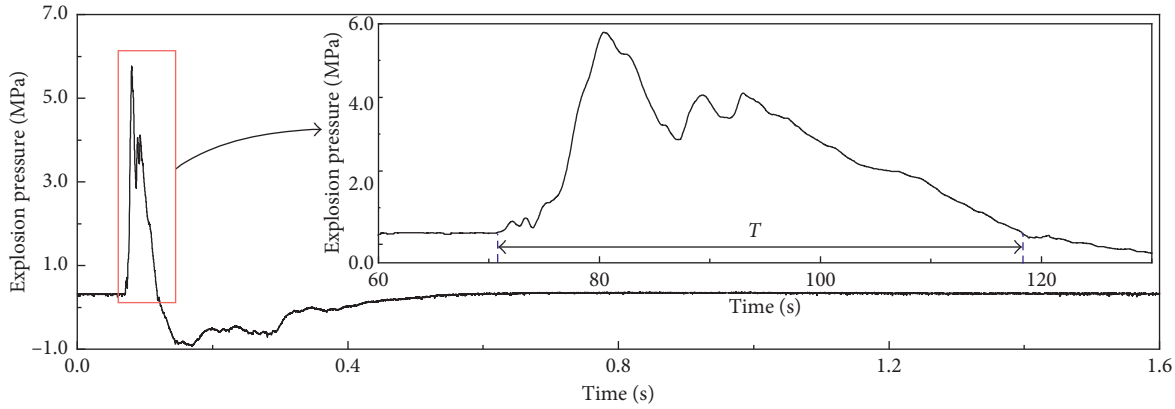

Figure 10: The change curve of external explosion pressure during the liquid carbon dioxide blasting.

oscillatory decrease in pressure. Because the explosion pressure outside the blasting pipe is controlled by the explosion pressure in the blasting pipe, it also decreases in an oscillatory pattern.

4. Liquid Carbon Dioxide Rock Breaking Experiment

4.1. Test Scheme for the Liquid Carbon Dioxide Rock Breaking Experiment. In order to research the rock breaking characteristics of liquid carbon dioxide blasting, a sample target was prepared with dimensions of 500 mm × 500 mm × 400 mm. It consisted of a ratio of 1 part 325# Portland cement : 1 part fine sand : 0.5 parts water. The blasting hole had a diameter and length of 45 mm and 200 mm, respectively. A structural diagram of the sample and the finished sample is shown in Figure 11. The arrows represent the jetting direction of the liquid carbon dioxide fracturing device. The corresponding experiment samples that were used to obtain the physical and mechanical parameters of the exploded sample were made at same time and have the same materials and proportions. After 28 days of maintenance, the indoor rock mechanics experiments

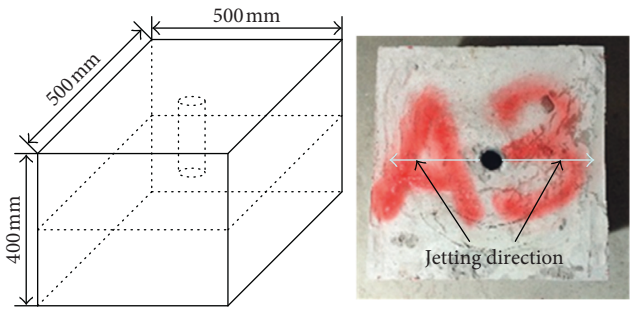

Figure 11: Structural diagram of the sample and image of the finished sample.

were carried out to obtain the physical and mechanical parameters of the exploded sample; these are shown in Table 2.

4.2. The Analysis of Experiment Results. Figure 12 shows that, after liquid carbon dioxide blasting, sample A3 suffered three main fractures; all of them penetrated through to the edges of the sample. Aside from these fractures, the hole wall

Table 2: The physical and mechanical parameters of the exploded sample.

Density ($\times 10^3$ kg/m^3)	Uniaxial compressive strength (MPa)	Uniaxial tensile strength (MPa)	Poisson ratio	Elastic modulus (GPa)	Cohesion (MPa)	Friction angle (°)
1.878	27.7	2.47	0.234	2.01	7.023	7.35

(a) (b)

Figure 12: The exploded A3 sample after liquid carbon dioxide blasting.

was largely intact, and there was no crushing area around the hole. This is in contrast to the use of explosives, which will form an obvious crushing area [29, 30]. These results indicate that liquid carbon dioxide blasting technology could fracture rock rather than crush rock and have a better fracturing effect than explosives. The entire sample damage surfaces were very smooth, showing that the failure mode of the specimen was tensile failure. This is mainly because of the effect of the high-pressure carbon dioxide gas on the exploded sample instantaneously after detonation, which resulted in the crack initiating and propagating. The carbon dioxide gas could then quickly penetrate into the crack. Under the "gas wedge effect" of carbon dioxide, the sample is damaged by tension.

The hole wall after the blasting is shown in Figure 13. This figure shows that the hole wall was largely undamaged and retained its shape after the liquid carbon dioxide blasting. However, the lower part of the hole wall, which was adjacent to the outlet location of the liquid carbon dioxide fracturing device, is relatively rough and has an obvious pit. The pit is narrow and long, and its orientation is perpendicular to the axial direction of the blasting. Its depth is about 0.7 mm. At the bottom of the blasting hole, there was a microcrack along the axial direction of blasting hole with a length of 7 cm. The trace of the microcrack is approximately straight, and there were no secondary microcracks in the surrounding area. This phenomenon also shows that the liquid carbon dioxide blasting technology has a good fracturing effect. The pit formed because the high-pressure carbon dioxide was released at a speed of a few hundred meters per second after blasting and formed into a gas jet, under the impact of which the pit was formed.

The smooth conical block formed under the blasting hole after blasting is shown in Figure 14, and the mechanism of its formation is shown in Figure 15. The hole wall was subjected to the repeated impact of high-pressure carbon dioxide, and the torque in the corner of the blasting hole was at its maximum. In addition, this part itself has obvious edges and corners, so it was particularly easy to form stress concentration. Under the dual action of these effects, the bottom of the blasting hole was especially easy to fracture and form the microcracks. The high-pressure carbon dioxide was then able to invade into these microcracks and cause the stress concentration in the microcrack tip. Coupled with the "gas wedge effect" of the high-pressure carbon dioxide, it appears that the microcracks have further developed into the macro tensile destroyed surfaces. Finally, the smooth conical block was formed. The formation of the smooth conical block also shows that the "gas wedge effect" of the high-pressure carbon dioxide plays a leading role in the rock breaking process.

5. Conclusion

(1) The entire process of liquid carbon dioxide blasting can be viewed as having three stages: liquid gasification of carbon dioxide, carbon dioxide release, and the recovery of the negative pressure zone. The explosion pressure in the fracturing device varied according to the law of "exponential followed by linear increase," "shock attenuation," and "parabolic growth," respectively. The duration times of gasification and the release of carbon dioxide were 70.04 ms and 46.4 ms, respectively. The maximum explosion pressure and the minimum explosion pressure were 104.62 MPa and −12.33 MPa, respectively.

(2) The duration time of the entire blasting effect stage was about 45 ms. During this time, the explosion pressure outside the blasting pipe increased exponentially and then attenuated in and oscillatory fashion. The liquid carbon dioxide blasting technology mainly uses the cyclic impact created by this oscillation to destroy the target object.

(3) The rock breaking characteristics of liquid carbon dioxide blasting technology are characterized by

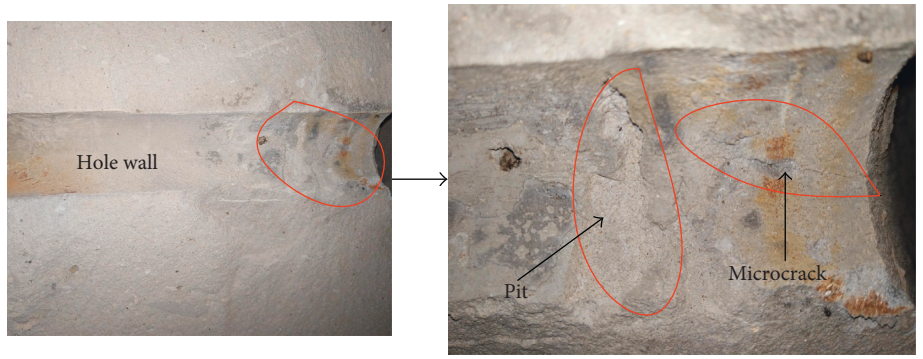

Figure 13: The hole wall after liquid carbon dioxide blasting.

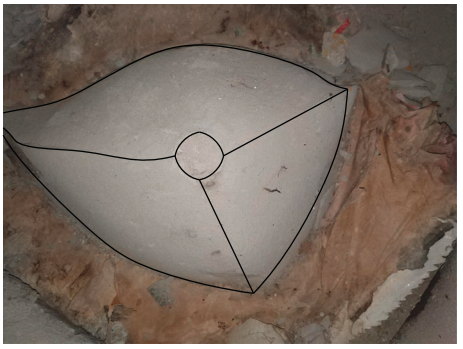

Figure 14: The smooth conical block after liquid carbon dioxide blasting.

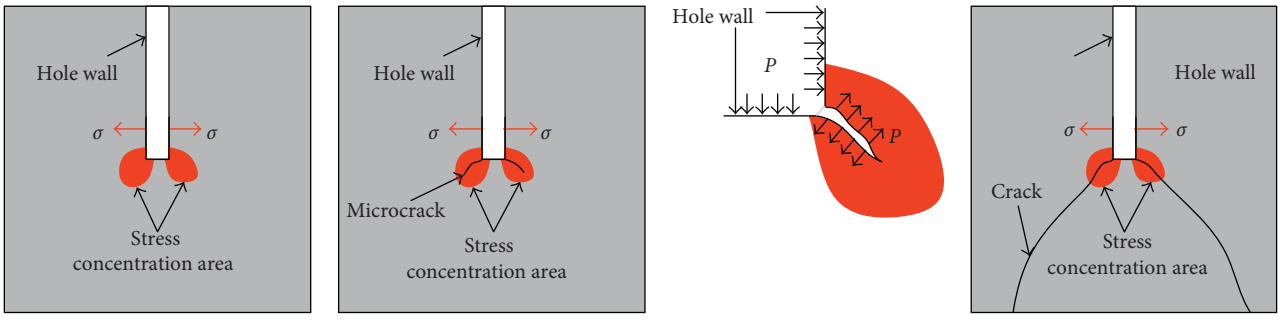

Figure 15: The formation mechanism of the smooth conical block. (a) Stress concentration. (b) Initiation of microcrack. (c) Development of microcrack. (d) Formation of conical block.

fracturing without crushing and jet impingement. The failure modes of the test specimens were mainly tensile failure and the "gas wedge effect." High-pressure carbon dioxide plays a leading role in the rock breaking process of liquid carbon dioxide blasting technology.

Data Availability

The data used to support the findings of this study are available from the corresponding author upon request.

Conflicts of Interest

The authors declare that there are no conflicts of interest regarding the publication of this paper.

Acknowledgments

The authors acknowledge the project (41502327) supported by the National Natural Science Foundation of China and the Fundamental Research Funds for the Central Universities of Central South University (2018zzts213).

References

[1] H. D. Chen, Z. F. Wang, X. E. Chen, X. J. Chen, and L. G. Wang, "Increasing permeability of coal seams using the phase energy of liquid carbon dioxide," *Journal of CO_2 Utilization*, vol. 19, pp. 112–119, 2017.

[2] N. Vidanovic, S. Ognjanovic, N. Ilincic, N. Ilic, and R. Tokalic, "Application of unconventional methods of underground premises construction in coal mines," *Technics Technologies Education Management*, vol. 6, no. 4, pp. 861–865, 2011.

[3] S. P. Singh, "Non-explosive applications of the PCF concept for underground excavation," *Tunnelling & Underground Space Technology*, vol. 13, no. 3, pp. 305–311, 1998.

[4] C. C. Fong, J. W. Altizer, V. E. Arnold, and J. K. Lawson, "Blasting machine utilizing sublimable particles," US Patent US4389820 A, 1983.

[5] F. Elbing, R. Rotstein, and M. Knackstedt, "Device and process for cleaning, activation or pretreatment of work pieces by means of carbon dioxide blasting," US Patent US7967664, 2011.

[6] D. H. Pickering, "Tests on cardox for the reinstatement of approval for use in coal mines," in *Proceedings of Industry Applications Society Annual Meeting*, pp. 251–259, Washington, DC, USA, 1989.

[7] W. X. Guo, *A Perfusion Machine for Filling the Carbon Dioxide Blasting Pile*, China, ZL201320575075.3, 2014, in Chinese.

[8] W. F. Yin, L. Shi, W. He et al., *A Carbon Dioxide Extractor with the Function of Stopping fly Self-Adaptive*, China, ZL201420224048.6, 2014, in Chinese.

[9] R. C. Miller, *Fundamental Study of Carbon Dioxide Blasting: An Experimental and Numerical Analysis of Surface Cleaning by a Particle-Laden Turbulent Jet*, Michigan Technological University, Houghton, MI, USA, 1995.

[10] R. Holmberg and T. White, "Cardox system brings benefits in the mining of large coal," *Coal international*, vol. 243, no. 1, pp. 31–33, 1995.

[11] G. M. Reimer, "Reconnaissance techniques for determining soil-gas radon concentrations: an example from prince Georges County, Maryland," *Geophysical Research Letters*, vol. 17, no. 6, pp. 809–812, 1990.

[12] K. P. Zhou, F. Gao, H. W. Gao, H. W. Deng, and J. L. Li, *A mining Method of Adopting Liquid Carbon Dioxide Blasting Technology to Induce Caving*, China, ZL201410798159.2, 2015, in Chinese.

[13] Z. X. Guo, "Liquid carbon dioxide blasting tube and field test blasting," *Blasting*, vol. 3, pp. 72–74, 1994, in Chinese.

[14] B. Wang, "Research on increasing permeability of coal seam by using CO_2 blasting technology," *Hydraulic Coal Mining & Pipeline Transportation*, vol. 2, pp. 9–11, 2015, in Chinese.

[15] H. D. Chen, Z. F. Wang, L. L. Qi, and F. H. An, "Effect of liquid carbon dioxide phase change fracturing technology on gas drainage," *Arabian Journal of Geosciences*, vol. 10, no. 14, p. 314, 2017.

[16] T. K. Lu, Z. F. Wang, H. M. Yang, P. J. Yuan, Y. B. Han, and X. M. Sun, "Improvement of coal seam gas drainage by underpanel cross-strata stimulation using highly pressurized gas," *International Journal of Rock Mechanics and Mining Sciences*, vol. 77, pp. 300–312, 2015.

[17] X. H. Zhou, J. L. Men, P. H. Wang, and G. Bai, "Industry experimental research on improving permeability by underground liquid CO_2 blasting," *Journal of Safety Science and Technology*, vol. 11, no. 9, pp. 76–82, 2015, in Chinese.

[18] J. Wang and Y. S. Xiao, "Marble stone is mined in a limestone mine based on carbon dioxide blasting technology," *Modern Mining*, vol. 554, pp. 15–17, 2015, in Chinese.

[19] Z. F. Wang, H. J. Li, X. E. Chen, L. Zhao, and D. C. Zhou, "Study on hole layout of liquid CO_2 phase-transforming fracture technology for permeability improvement of coal seam," *Journal of China Science and Technology*, vol. 11, no. 9, pp. 11–16, 2015, in Chinese.

[20] Q. X. Dong, Z. F. Wang, Y. B. Han, and X. M. Sun, "Research on TNT equivalent of liquid CO_2 phase-transition fracturing," *China Safety Science Journal*, vol. 24, no. 11, pp. 84–88, 2014, in Chinese.

[21] J. H. Kang, F. B. Zhou, Z. Y. Qiang, and S. J. Zhu, "Evaluation of gas drainage and coal permeability improvement with liquid CO_2 gasification blasting," *Advances in Mechanical Engineering*, vol. 10, no. 4, pp. 1–15, 2018.

[22] L. Ma, G. M. Wei, Z. B. Li, Q. H. Wang, and W. F. Wang, "Damage effects and fractal characteristics of coal pore structure during liquid CO_2 injection into a coal bed for E-CBM," *Resources*, vol. 7, no. 2, p. 30, 2018.

[23] R. H. Nilson, W. J. Proffer, and R. E. Duff, "Modelling of gas-driven fractures induced by propellant combustion within a borehole," *International Journal of Rock Mechanics and Mining Science and Geomechanics Abstracts*, vol. 22, no. 1, pp. 3–19, 1985.

[24] M. Goodarzi, S. Mohammadi, and J. Ahmad, "Numerical analysis of rock fracturing by gas pressure using the extended finite element method," *Petroleum Science*, vol. 12, no. 2, pp. 304–315, 2015.

[25] W. C. Zhu, D. Gai, C. H. Wei, and S. G. Wei, "High-pressure air blasting experiments on concrete and implications for enhanced coal gas drainage," *Journal of Natural Gas Science and Engineering*, vol. 36, pp. 1253–1263, 2016.

[26] Z. M. Zhu, B. Mohanty, and H. P. Xie, "Numerical investigation of blasting-induced crack initiation and propagation in rocks," *International Journal of Rock Mechanics and Mining Sciences*, vol. 44, no. 3, pp. 412–424, 2007.

[27] K. P. Zhou, B. Ke, J. L. Li et al., *A Carbon Dioxide Blasting Experiment Device*, China, ZL201520972630.5, 2016, in Chinese.

[28] Z. M. Zhu, H. P. Xie, and B. Mohanty, "Numerical investigation of blasting-induced damage in cylindrical rocks," *International Journal of Rock Mechanics and Mining Sciences*, vol. 45, no. 2, pp. 111–121, 2008.

[29] Z. M. Zhu, "Numerical prediction of crater blasting and bench blasting," *International Journal of Rock Mechanics and Mining Sciences*, vol. 46, no. 6, pp. 1088–1096, 2009.

[30] M. Li, Z. M. Zhu, R. F. Liu, B. Liu, L. Zhou, and Y. Q. Dong, "Study of the effect of empty holes on propagating cracks under blasting loads," *International Journal of Rock Mechanics & Mining Sciences*, vol. 103, pp. 186–194, 2018.